Aggregation of Silicon Nanocrystals Prepared by Laser Ablation in Deionized Water

Vladimir Švrček*, Takeshi Sasaki, Yoshiki Shimizu and Naoto Koshizaki

Nanoarchitectonics Research Center, AIST, Central 5, 1-1-1 Higashi, Tsukuba, Ibaraki 305 8565、Japan
E-mail: vladimir.svrcek@aist.go.jp

Luminescent silicon nanocrystals (Si-ncs) prepared in colloidal suspensions are a potentially very important material for future optoelectronics, biology, photonics etc. We report on fabrication of luminescent Si-ncs in deionized water. The Si-ncs were formed at room temperature by two different techniques: (1) red luminescent Si-ncs by electrochemical etching and pulverizing of porous silicon films, and (2) blue luminescent Si-ncs by laser ablation with various laser fluence ranging from 0.07 to 6 mJ/pulse. Our attention is focused on aggregation and aging of Si-ncs in deionized water. It was observed that fine Si-ncs were agglomerated into well-defined spheres at low laser fluence while the shock waves inhibited their formation at higher fluence. Aging in deionized water promoted aggregation of irregular Si-ncs fragments into larger spheres with keeping their Si bulk crystallinity.

DOI: 10.2961/jlmn.2007.01.0003

Keywords: Silicon nanocrystals, laser ablation, liquid medium.

1. Introductions

Well-dispersed semiconductor nanocrystals have attracted attention of research community in last decades as a zero dimensional nanostructure that can be directly applied into optoelectronics, biology, medicine etc. Silicon nanocrystals (Si-ncs) play a particular role among various semiconductor nanocrystals [1, 2, 3]. The reasons are multiple. Nowadays silicon-based technologies, such as photovoltaics and electronics, make silicon very accessible, demanding and relatively cheap. In addition, since Si-ncs have low toxicity and fully compatible with a human body, such a colloidal luminescent Si-ncs may also be preferable as a fluorescent labeling agent in biological systems when compared to other currently used materials. Many techniques have been applied to fabricate luminescent Si-ncs, though most of them can easily provide the red luminescent Si-ncs. To prepare the blue luminescent Si-ncs by cost-effective way remains still a challenge, especially in water as colloidal solution [4]. The blue luminescent Si-ncs compare to red ones can have additional advantages, i.e. decreased size, increased integration capacity and faster performance in nanotechnology devices.

Recently the pulsed laser ablation in liquid media has attracted significant attention as a novel technique for the fabrication of nanoparticle colloidal solution. The advantages are quite a few. For instance, we can easily control the experimental conditions, such as nanoparticle host ambiance and laser parameter, and most importantly the technique is applicable to a wide range of materials [5, 6]. In addition, ablation in water can open applications into biology and/or the fabrication of oxide nanomaterials without any post annealing. It is well known that nanoparticles a few nanometers in diameter are not stable in colloid suspensions and very often get stabilized into aggregates with different sizes and shapes.

However, it is crucial to understand the details of aggregation mechanisms because they can determine the nature of the surface states and therefore the properties of Si-ncs. In this work we compare properties of Si-ncs dispersed in deionized water as colloidal solution fabricated by following two independent techniques. (1) The Si-ncs were formed by electrochemical etching in hydrofluoric acid mixed with ethanol and pulverizing such prepared porous silicon wafers. (2) The Si-ncs were directly fabricated by nanosecond laser ablation in water using of crystalline silicon as a target. In particular our attention is focused on aggregation and fragmentation processes as a function of laser fluences.

2. Experimental details

To fabricate the Si-ncs by laser ablation we used crystalline silicon wafer (p-type, <100>, resistivity 0.1 ohm·cm, thickness 0.525 mm) as a target. A third harmonic Nd:YAG laser (Spectra Physics LAB-150-30, 355 nm, 30 Hz, 8 ns) was irradiated the onto a target immersed in 10 ml of deionized water at room temperature for 30 min. After focusing by lens, the laser spot diameter on the target was 1 mm. The laser fluences were varied from 0.07 to 6 mJ/pulse.

For comparison the red luminescent Si-ncs were prepared by pulverization method from porous silicon films [7]. The porous silicon films were fabricated by standard electrochemical etching of single-crystalline silicon wafers (p-type, <100>, resistivity 0.1 ohm·cm, thickness 0.525 mm) in a mixture of hydrofluoric acid with ethanol (volume ratio=1:4), current density 1.6 mA/cm^2, etching time 2 hours). After the electrochemical etching the layers were mechanically scratched to obtain fine powder. Following

procedures were adopted to remove large porous silicon grains still present in initial scratched powder. The scratched porous silicon powder was dispersed in ethanol and then left precipitated for 1 hour. Then supernatant liquid ethanol containing the fine Si-ncs was carefully transferred into plastic cup. To remove the ethanol, the colloidal dispersion was dried at 50 °C. Fine powders were used for further investigations.

The granulometric studies were performed by Symex Malvern Zeta Sizer Nano ZEN 35000 (laser wavelength 532 nm) for the Si-ncs dispersed in deionized water. In case of Si-ncs prepared by electrochemical etching, Si-ncs once dried were wetted by 5 drops (1 drop ~ 0.025 cm^3) of ethanol and subsequently put in deionized water for better dispersion. Then the colloid was treated in ultrasonic bath for 10 minutes.

Scanning electron microscope (SEM) images were captured with a Hitachi SI 4800 microscope with 30 kV acceleration voltage and a 2 nm point-to-point resolution.

High-resolution transmission electron microscopy (HR-TEM) was performed on a microscope with 200 kV acceleration voltage (JEOL, JEM 2010). A small droplet of the obtained colloidal solution was deposited onto a copper grid with carbon film for HR-TEM and SEM observations. A convergent incident electron beam was sometimes employed in the diffraction measurements to perform more localized analyses of Si nanoparticles.

A small amount of Si-ncs dispersed in water was dropped onto a quartz plate. Then x-ray diffraction (XRD) patterns of Si-ncs were obtained using a diffractometer (Rigaku RAD-C) with Cu Kα radiation (λ=0.1540562 nm). The PL measurements were performed at room temperature using a fluorophotometer (Shimadzu, RF–5300PC) with excitation by monochromatic light at 300 nm from an Xe lamp.

3. Experimental Results and Discussion

3.1. As prepared Si-ncs

The most important feature of Si-ncs is their visible PL at room temperature. It is well known that Si-ncs prepared by electrochemical etching and dispersed in water have typical PL peak in red spectral region [3, 7]. Also in our case, the typical broad PL spectra at room temperature were recorded with maxima located around 2 eV. It is generally accepted that this visible strong PL was assigned to both surface states and quantum confinement effect (less than 10 nm) [8]. In contrast, the Si-ncs prepared in deionized water by nanosecond laser ablation showed the blue PL with maximum around 3 eV, similar to the results recently reported [4]. We believe that the origin is similar to the case of Si-ncs prepared by electrochemical etching. In addition strong oxidation possibly took place immediately after formation in case of laser ablation in water. The oxidation in principle can leads to Si-ncs size decrease, local stress, opening of bandgap, and subsequent blue PL observation. However, oxide passivation of Si-nc surface states and defects in oxide layer can also effectively increase the PL intensity. Aging and oxidation might also influence both quantum size effect and surface states.

The question arises whether Si-ncs maintain an indirect optical gap as typical for bulk silicon. Our evaluation of optical bandgap from optical transmittance data indicated that both direct and indirect band gaps had similar values of 2.9 eV. However, a PL dynamics measurement has to be performed to decide what kind of gap such prepared Si-ncs have, and this will be reported later.

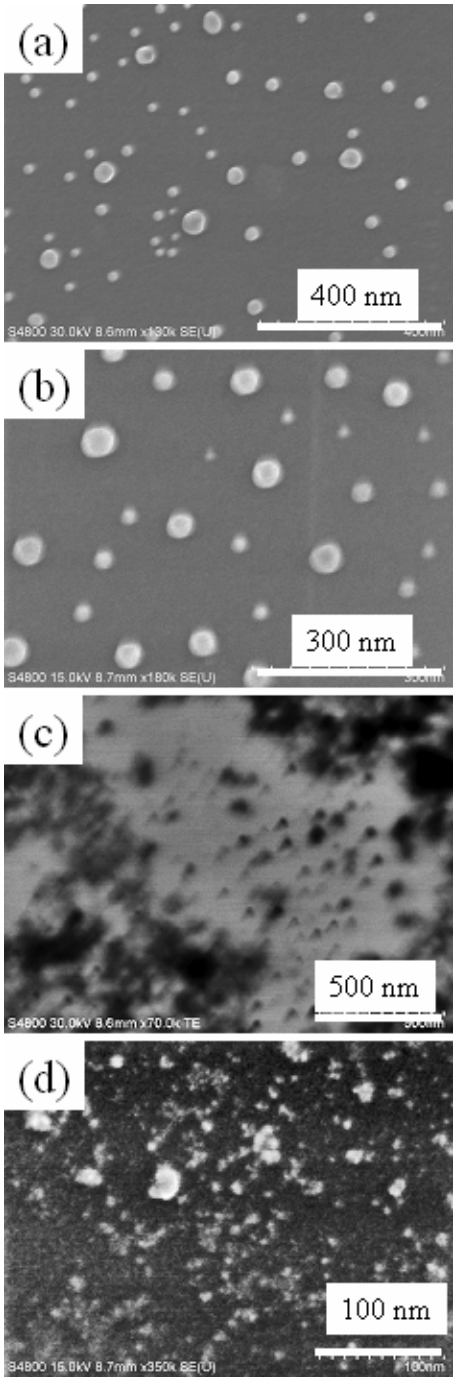

Fig. 1 SEM images of Si-ncs aggregates immediately after laser ablation of single-crystalline silicon target in deionized water with different laser fluences, (a) 0.07 mJ/ pulse, (b) 0.2 mJ/ pulse, (c) 1.1 mJ/ pulse and (d) 6 mJ/ pulse.

Figure 1 shows the SEM images of Si-ncs aggregates just after the preparation by laser ablation in deionized water with different laser fluences, (a) 0.07 mJ/ pulse, (b) 0.2 mJ/ pulse, (c) 1.1 mJ/p, and (d) 6 mJ/ pulse. As depicted in Figs. 1(a) and 1(b), we obtained spherical aggregates at low fluence with size distributions ranging from 2 to 100 nm. It was clearly observed that the smaller irregular aggregates of Si-ncs were obtained at higher fluence (≥1.1 mJ/ pulse) (Figs. 1(c) and 1(d)). At higher fluences the formation of spheres was inhibited mostly because of fragmentation processes. Such fragmentation is induced by the increased density and intensity of shock waves that propagate through liquid at higher laser fluences.

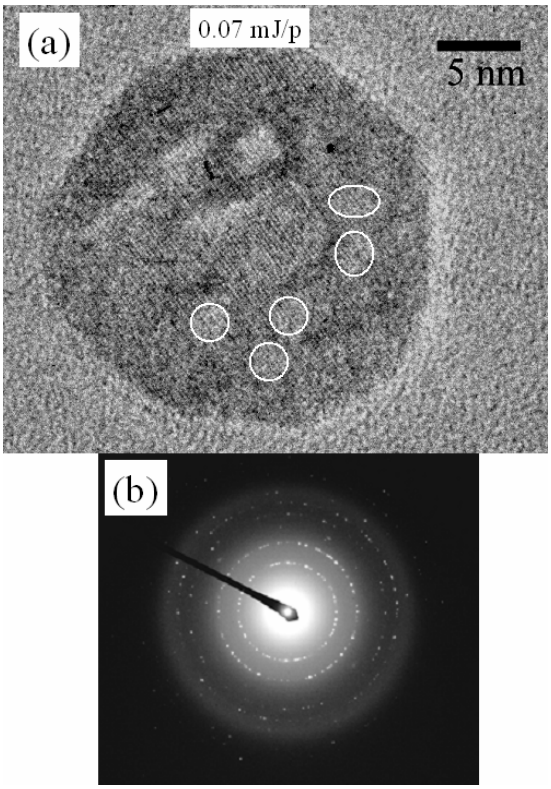

Fig. 2 (a) HR-TEM image of Si particle prepared at 0.07 mJ/p of laser fluence. The small Si-ncs with size 2-3 nm are shown in circles. (b) Corresponding electron diffraction analysis reveals the crystal structure of Si cubic phase.

HRTEM observation was performed to obtain more detailed information about structural properties of such regular spherical aggregates. A representative HR-TEM image of a sphere with 20 nm in diameter obtained at 0.07 mJ/pulse is presented in Fig. 2 (a). It can be seen that this spherical aggregate with the size of several nanometers was composed of separate Si-ncs (< 5 nm). It has to be noted that both spherical aggregates of Si nanoparticles obtained at lower fluences (Fig. 1(a)) and fragmented clusters in different shapes obtained at higher fluences (Fig. 1 (c, d)) had a Si cubic structure similar to bulk Si determined by electron diffraction (Fig. 2(b)) analysis. Ring diameters in Fig. 2(b) corresponded to the following crystalline silicon plane orientations: 3.146 Å for <111>, 1.93 Å <220>, 1.64 Å <311>, 1.34 Å <400>, 1.25 Å <331>, and 1.1 Å <422>.

Those results were further confirmed by XRD measurements. In XRD spectra three major peaks of crystalline silicon were clearly detected at 2θ=28.50°, 47.33°, and 56.17°, corresponding to the <111>, <220>, and <311>.

We also performed dynamic laser light scattering granulometric experiments to understand the detailed aggregation processes. The measurements were performed directly on a series of Si-ncs prepared in deionized water after ablation. It is well known that light scattering data can just provide qualitative information about the Si-ncs sizes, though it is well indicative of the aggregate sizes. Figures 3 (a)-(d) shows particle size distributions obtained from light scattering data of Si-ncs immediately after the preparation by laser ablation. Interestingly, two peaks in the size distribution curves were recorded for samples prepared at the fluences of 1.1 mJ/pulse or lower. Smaller Si-ncs aggregates were formed with the fluence increase. This tendency was also observed from SEM images. The largest aggregates about 1 μm in size were observed at 0.07 mJ/pulse, and the size decreased down to 270 nm with the fluence increase to 1.1 mJ/pulse. Only one peak is recorded at higher laser fluencie >2.4 mJ/pulse. The mechanism why we observe two peaks from light scattering measurements is not clear yet. The light scattering measurement represents secondary aggregate size immediately after preparation. Most probably at low laser ablation fluencies we form inhomogeneous secondary aggregates within the liquid media. Then the aggregates shown in Fig. 1(a-b) naturally tend to group into larger secondary aggregates with two distinguished diameters (Fig. 3 (a-b)). Both are stable mainly because of negative zeta potential (Fig.4b) and consecutive repulsion forces that inhibit them stick each other. At higher fluencies formation smaller particles (Fig. 1(d)) is favored and regular spherical aggregates are inhibited by mostly shock waves propagated through the liquid media. In addition, the shock waves can induce the fragmentation weakly attached Si particles [9]. This then leads to formation of smaller secondary aggregates with relatively homogenous size distribution as shown in Fig. 3(d). The larger specific surface of many smaller particles increases also the number of oxygen vacancies [10] and the zeta potential. As consequence repulsive forces decrease leads theirs stabilization into smaller aggregates around one diameter in average (Fig. 3(d). The results are summarized in Fig. 4 (a) the blank circles corresponds to peak 1 and triangles to peak 2. The light scattering experiment supported the tendency already observed by SEM, namely that aggregate size decreased with the fluences. The curve in Fig 4 (a) is a guide for eyes that indicates this decrease.

It has to be note that the zeta potential is the electrical potential that exists at the "shear plane" of a particle, which is some small distance from its surface. Aggregations are suppressed when absolute value of zeta potential exceeds well above 50 mV [11, 12]. In our experiments, the zeta potential considerably increased from large negative value (-29 mV at 0.07 mJ/pulse) to almost zero (-0.007 mV at 6 mJ/ pulse) with the laser fluence increase, as depicted in Fig. 4 (b). The zeta potential for all series was negative. The negative value results from many factors as particle environment, pH of solution etc. [10]. However, most important feature in our experiment is its absolute value

changes as a function of laser fluencies. One can expect that increased ablation intensity lead to the increase of particle specific surface area due to smaller aggregates with irregular shapes that in principle can contain larger number of oxygen vacancies located around Si-ncs resulting in an observed abrupt increase of the zeta potential (see Fig. 4(b)).

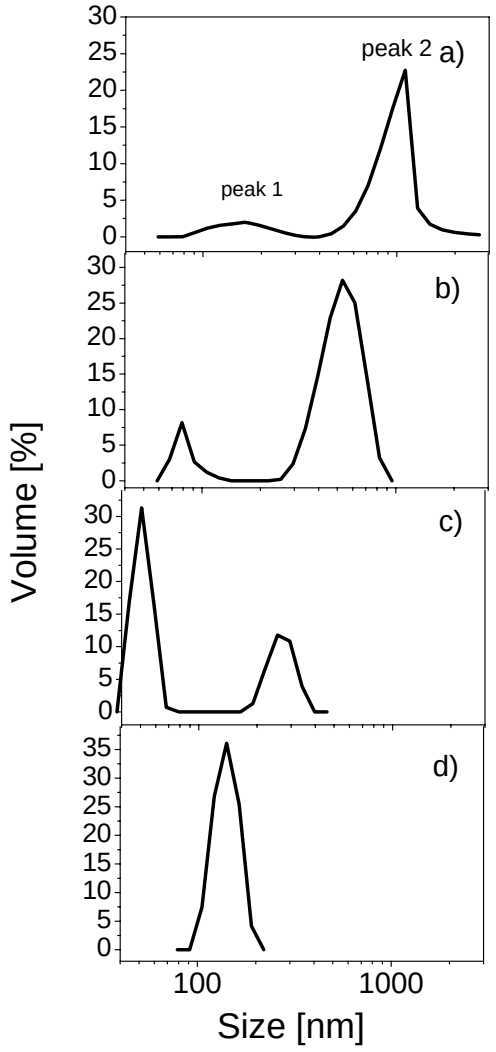

Fig. 3 Light scattering of Si-ncs aggregates prepared at different laser fluence in deionized water measured immediately after laser ablation at (a) 0.07 mJ/pulse, (b) 0.2 mJ/pulse, (c) 1.1 mJ/pulse, and (d) 2.4 mJ/pulse.

In the case of Si-ncs prepared by electrochemical etching, Si-ncs were continuously exposed to air during the collection process and therefore even before introducing into deionized water they are naturally embedded in SiO_x [13]. The Si-ncs are hydrophobic and become stabilized by an aggregation process. In this case the measured data are shown in Fig. 4. For example in the case of ablation at 6 mJ/pulse the as prepared aggregate sizes around 30 nm and zeta potential was about ~0.007 mV. Small absolute value of zeta potential was probably due to oxygen vacancies and large specific surface area similar to Si-ncs prepared by laser ablation at higher fluences as discussed above.

In spite of extensive investigations [14, 15], the ablation mechanism of water containing media remains unclear especially for silicon [16-18]. Basically, the analytical models predicted that laser-induced pressures in the water-confined ablation mode were based on three different phases occurring for the plasma: laser heating, adiabatic cooling, and final expansion. The model enabled to estimate the pressure inside the confined plasma plume [19]. Optical absorption ($>E_{gSi}$=1.1 eV) of nanosecond laser pulses in Si wafers led to rapid heat generation. Immediately after the laser ablation, a dense cloud of Si atoms was spread over the laser spot, i.e. the plume formation on a silicon wafer. In such a cloud, embryotic particles were also formed. Next, subsequent rapid aggregation of Si atoms onto embryotic particles continued until the nearby Si atoms were completely consumed. As the particles entered liquid medium from plume, the growth was suppressed. When Si-ncs entered deionized water, the surface was naturally covered with SiO_x shells that suppressed the Si-nc growth and subsequent stabilization by aggregation. Well-defined spheres at low fluence and irregular fragments at high fluence were thus formed (Fig. 1).

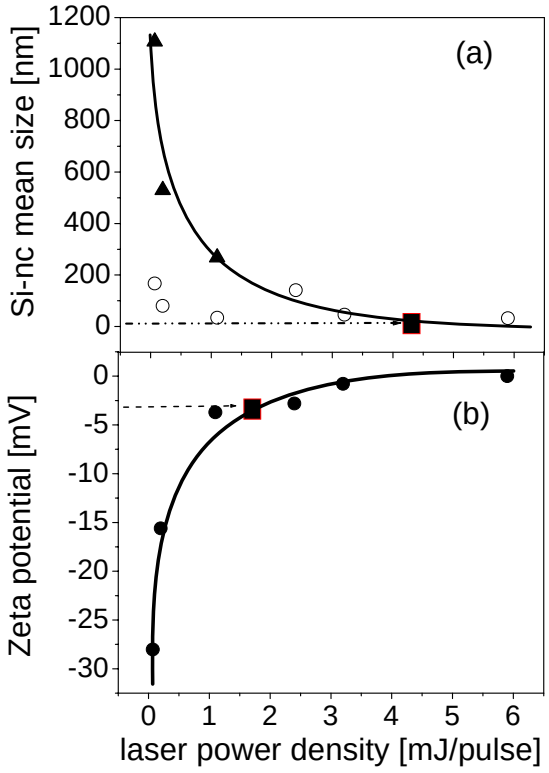

Fig. 4 (a) Blank circles and triangles represent aggregate average size corresponding to peak 1 and peak 2 in figure 3. (b) Corresponding zeta potential of as-prepared Si-ncs as a function of laser fluence for laser ablation in deionized water obtained by laser scattering analysis. Squares indicate the values for Si-ncs prepared by electrochemical etching.

3.2. Aging in the deionized water

Si-ncs and/or Si-ncs aggregates have to be stable in colloidal suspension in a long time for various application. It is well known that water itself is a strong oxidation agent. One can ask at least two questions concerning Si-ncs in water. How the water will affect the stability and properties of such Si-ncs aggregates in a long term. We have studied aging effects of such prepared Si-ncs aggregates by leaving them in deionized water at ambient temperature for six months. Typical SEM images of the same Si-ncs aggregates after six months of aging are shown in Fig. 5. Figure 5(a) shows Si-ncs aggregates prepared by laser ablation in water at the laser fluence of 0.07 mJ/pulse and aged for six months. As-prepared aggregates had spherical shape with the maximum size of 100 nm (see Fig. 1(a)), while after six-month aging the size increased to 350 nm more than three times of initial size (Fig. 5(a)). Thus the as-prepared small Si-ncs aggregates obtained at low laser fluences further aggregated into larger spheres by six-month aging.

Figure 5(b) depicts an SEM image of aggregates prepared at 6 mJ/p and aged for six months. At higher laser fluence (> 1.1 mJ/ pulse), by attaching the irregular Si-ncs aggregates (see Fig 1(d)) are formed and the spheres of 140 nm in average diameter are observed. One can speculate that at higher fluences smaller Si-ncs aggregates with irregular shapes were less stable and get stabilized into energetically favorable well-defined spheres. However, so far this phenomenon was not yet observed.

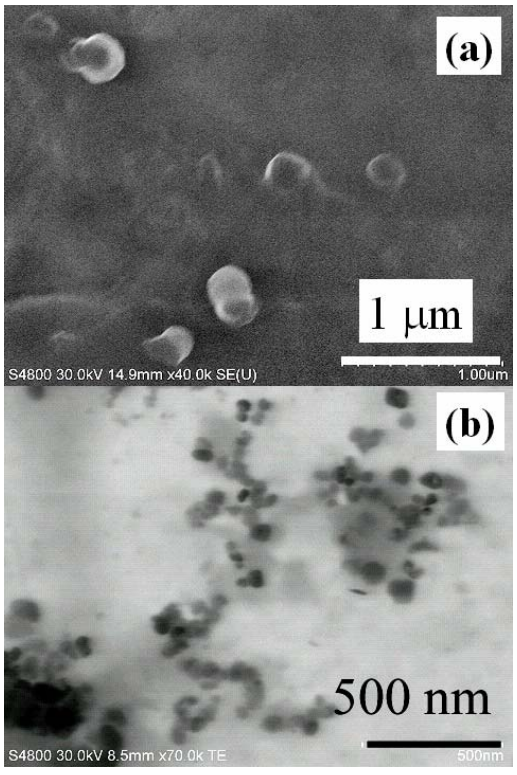

Fig. 5 Typical SEM images of Si-ncs aggregates after six months of aging in deionized water fabricated by laser ablation in deionized water at the laser fluence of (a) 0.07 mJ/pulse, and (b) 6 mJ/pulse.

The granulometric studies of Si-ncs after six-month aging are shown in Fig. 6. It has to be stressed that after aging we recorded just one peak for size distribution of Si-ncs aggregates dispersed in water. Mean aggregate size of Si-ncs versus laser fluence is summarized in Fig. 6(a). The mean aggregate size Si-ncs prepared at 6 mJ/pulse increased from 30 nm to 140 nm by aging. The mean size of aged Si-ncs aggregate decreased with increased laser fluence similar to the as-prepared Si-ncs aggregates, though the decrease is less abrupt (Fig. 6(a)). The difference between largest (6 mJ/pulse) and smallest (0.07 mJ/pulse) aggregate sizes of as-prepared Si-ncs was 1 μm, while that of aged Si-ncs was 100 nm.

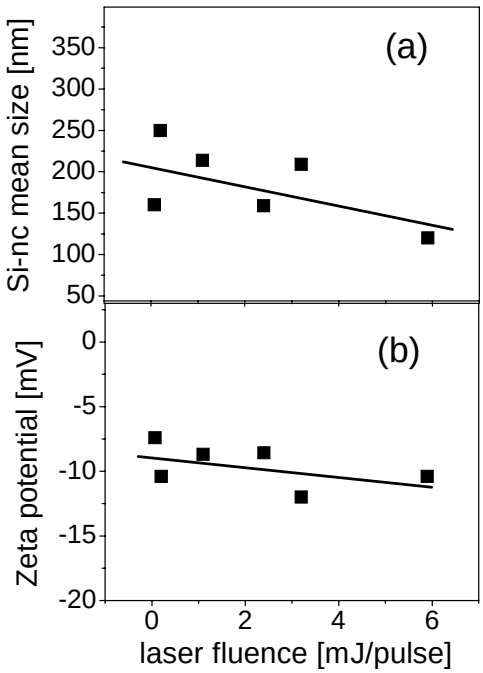

Fig. 6 (a) Aggregate size and (b) zeta potential of Si-ncs prepared by laser ablation and aged for six months in deionized water as a function of laser fluence obtained by laser scattering analysis.

The zeta potential slowly decreased (Fig. 6(b)) with laser intensity for aged Si-ncs compared to the as-prepared nanoparticles where it clearly increased with laser intensity (Fig. 4(b)). However, the zeta potential for all series was always negative similar to the as-prepared. This is probably due to the oxygen vacancies that still remained. The increased value of zeta potential at higher laser fluences can indirectly indicate that some of the oxygen vacancies were relaxed.

The question whether the Si-ncs after six-month aging in water keep their crystallinity arises. Our preliminary XRD measurements indicated that three major peaks of crystalline silicon were clearly detected at $2\theta = 28.50°$ for <111>, 47.33° for <220>, and 56.17° for <311>. However, more local structural studies are necessary to clearly investigate this issue, and will be reported soon.

4. Conclusions

In conclusion, we discussed two procedures for preparing luminescent ultra fine Si-ncs in deionized water. Red luminescent Si-ncs were prepared by pulverizing of porous silicon wafers, and blue luminescent Si-ncs were fabricated by nanosecond pulsed-laser ablation at room temperature in deionized water. It is observed that well-separated and spherical Si-nc aggregates were formed at low laser fluences. Laser fluence increase led to the fragmentation of spherical aggregates and the subsequent generation of smaller irregular Si-ncs aggregates. By six-month aging in the deionized water such irregular fragments were further aggregated into regular spheres adhered each other. In both cases of before and after aging the Si-ncs showed silicon cubic crystalline structure. We believe that such direct cost-effective approaches for nontoxic luminescent colloidal Si-ncs can provide important implications for wide field applications.

Acknowledgments
This work was partially supported by a JSPS fellowship. This study was also partially supported by the Industrial Technology Research Grant Program 2005 from the New Energy and Industrial Technology Development Organization (NEDO) of Japan.

References

[1] L. Pavesi, L. Dal Negro, L. Mazoleni, G. Franzo and F. Priolo, Nature **408,** (2000) 440.
[2] L. T. Canham, Appl. Phys. Lett. **57,** (1990) 1046.
[3] Y. Kanemitsu, Physics Reports **263,** (1995) 1-91.
[4] I. Umezu, H. Minami, H. Senoo, and A. Sugimara, in *8th International Conference on Laser Ablation (COLA 05)*, Banff, Canada, 2005, p. 268.
[5] F. Mafuné and T. Kondow, Chem. Phys. Lett. **343**, 383 (2004).
[6] T. Tsuji, K. Iryo, H. Ohta, and Y. Nishimura, Jpn. J. Appl. Phys. **39**, (2000) 981.
[7] V. Švrček, A. Slaoui, and J.-C. Muller, J. Appl. Phys. **95,** (2004) 3158.
[8] M. V. Wolkin, J. Jorne, P. M. Fauchet, G. Allan, and C. Delerue, Phys. Rev. Lett. **82**, (1999) 197.
[9] V. Švrcek, T. Sasaki, T. Shimizu and N. Koshizaki, Chem. Phys. Lett. **429,** (2006) 483
[10] H. Usui, T. Sasaki, N. Koshizaki, J. Phys. Chem. B **110,** (2006) 12890
[11] J. H. Lyklema Fundamentals of Interface and Colloid Science, Academic Press, London (1991)
[12] B.J. Kirby and E. F. Hasselbrick Electrophoresis 25, (2004) 187 .
[13 V. Švrček, A. Slaoui, J.-L. Rehspringer, and J.-C. Muller, Semicond. Sci. Technol. **20**, (2005) 314.
[14] R. E. W. Herrmann, J. Gerlach, and F. F. B. Campbell, Appl. Phys. A **66**, **(**1998) 35.
[15] P. Lorantzo, L. J. Lewis, and M. Meunier, Phys. Rev. Lett. **91**, (2003) 225502.
[16] D. Albagli, L. T. Perelman, G. S. Janes, C. V. Rosenberg, L. Itzkan, and M. A. Feld, Lasers Life Sci. **6**, **(**1994) 55.
[17] A. A. Oraevsky, V. S. Letoshkov, and R. O. Esenafiev, *Proceedings of the Workshop "laser ablation: Mechanism and Applications", Pulsed laser ablation of biotissue. review of ablation mechanisms* (Springer, Berlin, 1991).
[18] F. Partovi, J. A. Izatt, R. M. Cothren, C. Kittrell, J. E. Thomas, S. Strickwerda, J. R. Kramer, and M. S. Feld, Lasers Surg. Med. **7**, (1987) 141.
[19] R. Fabro, J. Fournier, P. Ballard, D. Devaux, and J. Virmont, J. Appl. Phys. **68,** (1990) 775.

(Received: May 16, 2006, Accepted: January 11, 2007)